Journal of Molecular Graphics and Modelling 53 (2014) 48–58

Contents lists available at ScienceDirect

Journal of Molecular Graphics and Modelling

journal homepage: www.elsevier.com/locate/JMGM

Interaction energy analysis on specific binding of influenza virus hemagglutinin to avian and human sialosaccharide receptors: Importance of mutation-induced structural change

Satoshi Anzaki[a], Chiduru Watanabe[b], Kaori Fukuzawa[b,c,1], Yuji Mochizuki[b,d], Shigenori Tanaka[a,*]

[a] Graduate School of System Informatics, Kobe University, 1-1, Rokkodai, Nada-ku, Kobe 657-8501, Japan
[b] Institute of Industrial Science, The University of Tokyo, 4-6-1, Komaba, Meguro-ku, Tokyo 153-8505, Japan
[c] Mizuho Information and Research Institute Inc., 2-3, Kanda Nishi-cho, Chiyoda-ku, Tokyo 101-8443, Japan
[d] Department of Chemistry and Research Center for Smart Molecules, Faculty of Science, Rikkyo University, 3-34-1, Nishi-Ikebukuro, Toshima-ku, Tokyo 171-8501, Japan

ARTICLE INFO

Article history:
Accepted 7 July 2014
Available online 18 July 2014

Keywords:
Influenza
Hemagglutinin (HA)
Mutation
Receptor binding
Fragment molecular orbital (FMO) method

ABSTRACT

On the basis of available molecular structures registered in Protein Data Bank, we have theoretically carried out the interaction energy analysis for the complexes of influenza virus hemagglutinin (HA) proteins and sialosaccharide receptor analogs of host cells. Employing the fragment molecular orbital method for quantum-chemical calculations, the differences in magnitude and pattern of the interactions between the amino acid residues of avian-type (H7N3) or human-type (H7N9) HA and each saccharide part of avian or human receptor were studied in order to elucidate the molecular mechanism of avian-to-human infectious transmission of influenza virus. We have thus confirmed quantitatively that the mutations from the avian HA to the human HA significantly strengthened the binding affinity of human HA to human receptor, while retaining the affinity to avian receptor. In addition to direct effects regarding the changes of interactions between the altered residues and the receptors, we have also found the importance of indirect effects in which structural changes caused by the mutations play vital roles to modify the intermolecular interactions.

1. Introduction

Hemagglutinin (HA), a spike-shaped, surface glycoprotein of the influenza virus, plays an important role in the early stage of infection through specific binding to the receptors (sialic acids) on the host cells and subsequent trigger for the fusion between virus and endosome membranes [1–5]. Thus, the investigation of the binding properties of HA with the pertinent saccharide receptors is essential for the elucidation and prediction of the influenza virus infection into animals and human beings [6–10]. In earlier studies [11,12], we have carried out the electronic-state calculations for a number of HA-receptor complex systems on the basis of the fragment molecular orbital (FMO) method [13–19], and found that the interaction energy analysis on molecular recognition between amino acid residues of HAs and saccharide receptors was very useful for elucidating the molecular mechanism of HA-receptor binding specificity.

In 2013, an avian-origin human-infecting influenza virus of H7N9 type was identified in China [20,21]. The receptor-binding properties of the viral HAs of human-infecting H7N9 isolates were then evaluated [22] and compared [23] with those of an avian H7N3 virus. It was thus found in the case of A/Anhui/1/2013 virus [23] that the HA of this human H7N9 virus had a significantly higher affinity for α-2,6-linked sialic acid analog (human receptor) than the HA of an avian H7N3 virus (A/Turkey/Italy/214845/2002), while retaining the strong binding to α-2,3-linked sialic acid analog (avian receptor). Since the X-ray crystal structures of the H7N9 and H7N3 HAs in complex with the avian and human receptor analogs are available [22,23], it is interesting to perform a theoretical study concerning the mechanism of specific binding or molecular recognition between HAs and receptors through the FMO electronic calculations, which could elucidate the molecular mechanism of how the mutated HA of H7N9 virus has become able to bind human receptors while still retaining the avian-receptor binding property.

* Corresponding author. Tel.: +81 78 803 6620; fax: +81 78 803 6621.
E-mail address: tanaka2@kobe-u.ac.jp (S. Tanaka).
[1] Present address: School of Dentistry at Matsudo, Nihon University, 2-870-1, Sakae-cho-nishi, Matsudo, Chiba 271-8587, Japan.

http://dx.doi.org/10.1016/j.jmgm.2014.07.004
1093-3263/

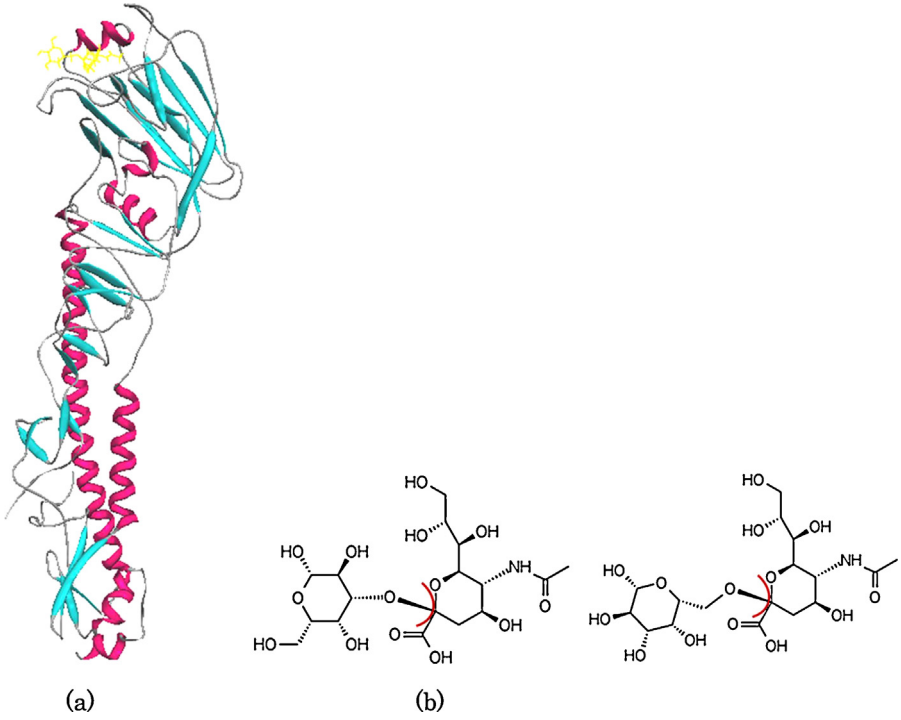

Fig. 1. (a) X-ray crystal structure of the complex of A/Anhui/1/2013 (H7N9) HA and human receptor (PDB entry: 4KON). The receptor (sialosaccharide) part is denoted by yellow color. (b) Schematic view of the fragmentation for the sialosaccharide chain.

The purpose of the present study is hence to theoretically analyze the molecular mechanism of the avian-to-human infectious transmission of the H7N9 influenza virus through the quantum-chemical calculations for the binding specificity and molecular recognition of HA-receptor complexes on the basis of the FMO method. We employ the X-ray crystal structures [22,23] of the complexes between the HAs of H7N9 (human) or H7N3 (avian) virus and the avian or human receptor analogs, which would significantly reduce the computational inaccuracies due to the uncertainties of molecular structures. In the following, we first explain the computational details of the FMO method in Section 2. Next we show in Section 3 the calculated results, which will demonstrate to what extent the direct interactions between the mutated amino acid residues and the receptors are altered, and then will reveal the importance of an indirect effect due to the structural changes caused by the modifications of intermolecular and intramolecular interactions associated with the point mutations. Concluding remarks are given in Section 4, where we address a possible contribution of the present study to the elucidation and prediction of probable interspecies transmission that may be associated with influenza pandemic.

2. Materials and computational methods

We employed X-ray crystal structures of complexes of HA protein (H7N3 or H7N9 type) and human or avian receptor [22,23]. Their PDB codes are 4BSH (H7N3 and human receptor 6′SLN), 4BSI (H7N3 and avian receptor 3′SLN), 4KON (H7N9 and human receptor 6′SLNLN) and 4KOM (H7N9 and avian receptor 3′SLNLN), where the H7N3 and H7N9 type HAs are regarded as hemagglutinin proteins of avian and human infection type, respectively. The resolutions of these X-ray diffraction data are similar, ranging between 2.25 and 2.62 Å. Fig. 1(a) illustrates the molecular structure of 4KON. Hydrogen atoms were added to these complexes by the MOE (Molecular Operating Environment) software (Chemical Computing Group Inc.), and their positions were optimized with the Amber99 force field [24].

The FMO calculations [11,12,15,18,19] with the software ABINIT-MP were performed for these complexes, where we employed the Hartree–Fock (HF) and the second-order Møller–Plesset (MP2) perturbation methods with the basis set of 6-31G. While the HF method is a mean-field type approximation, the MP2 perturbation method is employed for the description of electron correlations in the present study, where the latter is expected to take into account the dispersion (or van der Waals) interactions appropriately [19]. There is another problem about the quality of the basis set. Actually, the basis set of 6-31G may be too small to accurately describe the interaction energies in biomolecular systems. It has been found, however, that the FMO-IFIE analyses by the 6-31G, 6-31G* and 6-31G** basis sets have provided very similar results concerning the ligand–receptor interactions [25]. In addition, the counter-poise correction for the basis set superposition error has recently been performed in the context of FMO-IFIE analysis [26], which has led to consistent results between the corrected and uncorrected IFIE values to infer the relative significance of each fragment interaction. Thus, it is supposed that we can quantitatively evaluate the binding energy in terms of the present MP2 method (see also comprehensive literature [27]). Concerning the comparison to the interaction energy analysis in terms of classical force field (*e.g.*, AMBER, CHARMM and OPLS) [28], see also the Supplementary Information.

It is remarked that the effective fragment–fragment interactions in the FMO scheme are obtained in terms of the inter-fragment interaction energy (IFIE) [11,12,19,25,26,29–31] that is defined as

$$\Delta E_{ij} = (E'_{ij} - E'_i - E'_j) + \mathrm{Tr}(\Delta P_{ij} V_{ij}), \quad (1)$$

where ΔP_{ij} is a difference density matrix, V_{ij} is an environmental electrostatic potential for fragment dimer *ij* from other fragments, and E'_i and E'_{ij} are energies of fragment monomer i and dimer *ij* without environmental electrostatic potential, respectively. These values ΔE_{ij} then represent the effective interaction energies of an

amino acid residue with a ligand or between amino acid residues because each amino acid is treated as a single fragment in the present analysis [11,12,19,25,26,29–31]. The IFIEs are thus calculated in this study to analyze the interaction pattern and to estimate the contribution of each residue to binding, as seen below. In addition, each sugar moiety of receptors is treated as a single fragment (see Fig. 1(b)) [11,12,19].

It is also convenient to introduce [11,15,19]

$$\Delta E_{IJ}^{\text{total}} = \Sigma_j \Delta E_{ij}, \tag{2}$$

which refers to the contribution of each fragment i to the binding affinity with the domain J containing the grouped residues j. It is noted here that

$$\Delta E_{IJ}^{\text{total}} = \Sigma_i \Delta E_{ij}^{\text{total}} \tag{3}$$

represents the inter-domain interaction between the domain I containing the residues i and the domain J containing the residues j. All these calculations were carried out in this work up to the level of the two-body FMO expansion, *i.e.*, FMO2 [19]. It is expected [32] that the higher-order expansions such as FMO3 [19] do not alter the conclusions of this work.

In the present study, all the FMO calculations were performed *in vacuo*. It may be remarked that the inclusion of solvent effects would be important to quantitatively evaluate the inter-fragment interaction energies. However, as has been investigated in the literature [15,19,25,33], the relative importance of the contributions of each residue to the protein–ligand interactions would not be affected significantly if the comparison among the same kind (charged, polar or hydrophobic) of amino acid residues is carried out. This is a reason why we relied on the FMO-IFIE analysis *in vacuo*, while the development of FMO methods with inclusion of solvent and screening effects [16,19,34,35] is currently in progress. In addition, the inclusion of the entropic effects upon protein–ligand binding and conformational sampling would improve the consistency with experimental binding affinity or free energy, even through semiempirical corrections [36,37].

3. Results and discussion

3.1. Effects of mutations on the binding affinity between HA and saccharide receptor

Before going into the interaction energy analysis, we first make a comparison of amino acid sequences among three types of HAs. In addition to avian H7N3 (A/Turkey/Italy/214845/2002) [23] and human H7N9 (A/Anhui/1/2013) [23] types, we also employed avian H7N7 (A/Netherlands/219/2003) type HA [38], which showed highly pathogenic human infections in 2003. We have carried out a sequence alignment for these HAs with ClustalW [39], as seen in

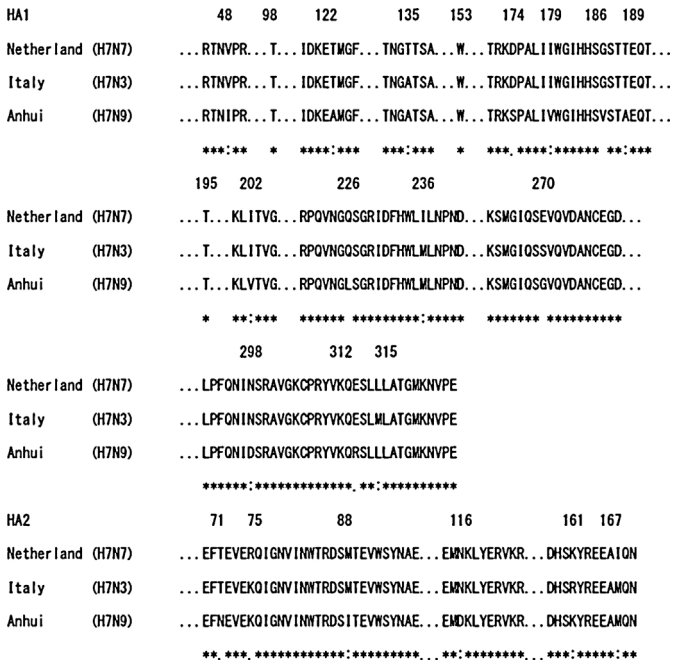

Fig. 2. Sequence alignment of amino acid residues of HAs among H7N7 (A/Netherlands/219/2003), H7N3 (A/Turkey/Italy/214845/2002) and H7N9 (A/Anhui/1/2013) influenza viruses.

Fig. 2. As for H7N9 (Anhui), it is observed that 14 of 476 residues have mutated, while other residues are conserved in comparison with other H7 type HAs. Considering the important roles of 130-loop, 190-helix, 220-loop, Tyr98, Trp153, His183 and Tyr195 supposed for the binding to saccharide receptors [40], we here pay attention to those mutations such as G186V, T189A, Q226L and D174S observed in H7N9, three of which are mutations into hydrophobic residues.

Table 1 lists the interaction energies between H7N3 or H7N9 type HA and parts (SIA1, GAL2, NAG3 and GAL4, where SIA, GAL and NAG refer to sialic acid, galactose and N-acetyl glucosamine, respectively) of avian or human receptor obtained by the FMO calculations on the basis of Eqs. (1)–(3). It is noted here that the avian and human receptors are characterized by the α-2,3 and α-2,6 linkages between SIA1 and GAL2 [41]. As observed in this table, the human HA (H7N9) shows weaker attractive interactions with the avian receptor than the avian HA (H7N3), but even the former still keeps a moderate binding to the avian receptor. The human HA, H7N9 (Anhui), which may be regarded as a mutant from avian HA, shows a significantly stronger binding to the human receptor than to the avian receptor. The former binding is stronger than that

Table 1
IFIEs (in units of kcal/mol) between HAs of H7N3 or H7N9 and each part of saccharide receptors. (a) Avian receptor and (b) human receptor. Sums of each contribution are also shown.

(a)

	SIA1	GAL2	NAG3	GAL4	Sum A (SIA1 + GAL2 + NAG3)	Sum A + GAL4
H7N3 (avian)	−188.8	−3.8	2.0		−190.6	
H7N9 (human)	−186.3	0.6	6.4	−1.8	−179.3	−181.1
ΔIFIE	−2.5	−4.4	−4.4		−11.3	

(b)

	SIA1	GAL2	Total (SIA1 + GAL2)
H7N3 (avian)	−183.6	−3.0	−186.6
H7N9 (human)	−204.2	0.9	−203.3
ΔIFIE	20.6	−3.9	16.7

Values in kcal/mol.

Table 2
IFIEs (in units of kcal/mol) between each amino acid residue of H7N3 (avian) HA and each part of avian receptor. (a) SIA1, (b) GAL2 and (c) NAG3. The MP2 value is given by the sum of the HF value and the correlation correction. Only the important interactions whose magnitudes are large or which play a vital role for binding are shown along with the charged state of the residues. See also Fig. S1 in Supplementary Information.

Residue	Charge	HF	Correlation	MP2
(a)				
ASP77	−	18.6	0.0	18.6
ASP95	−	16.3	0.0	16.3
TYR98		−12.2	−3.9	−16.0
LYS101	+	−20.2	0.0	−20.2
ARG131	+	−27.4	−0.1	−27.4
THR136		−27.2	−7.6	−34.8
SER137		−33.4	−3.4	−36.8
ARG140	+	−25.8	0.0	−25.8
ARG141	+	−24.9	0.0	−24.9
LYS152	+	−17.6	0.0	−17.6
ASP158	−	28.6	0.0	28.6
GLU190	−	20.3	−2.6	17.6
LYS193	+	−37.2	−0.1	−37.4
LYS200	+	−17.7	0.0	−17.7
ARG220	+	−25.9	0.0	−25.9
ARG229	+	−32.1	−0.1	−32.2
ASP231	−	18.9	0.0	18.9
ASP255	−	15.0	0.0	15.0
ALA135		1.2	−1.7	−0.5
GLN226		16.3	−3.4	12.9
(b)				
ARG131	+	1.5	0.0	1.5
THR136		−1.6	−0.2	−1.7
SER137		1.4	0.0	1.3
GLU190	−	3.1	−1.8	1.3
GLN191		−1.0	0.0	−1.0
GLN226		−2.9	−2.0	−5.0
(c)				
SER137		0.6	0.0	0.6
GLU190	−	−2.6	0.0	−2.6
LYS193	+	1.0	0.0	1.0
ARG220	+	0.9	0.0	0.9
ARG229	+	0.7	0.0	0.7

Values in kcal/mol.

between the avian HA (H7N3) and the avian or human receptor. In the following, we will perform molecular level studies on these issues in more details.

3.2. Interactions between HA proteins and avian receptor

In this section we consider the interactions between the HA proteins and the avian type α2–3 receptor. Table 2 and Fig. S1 (in Supplementary Information) illustrate the IFIEs between amino acid residues of avian (H7N3) HA and each part (SIA1, GAL2 and NAG3) of avian receptor. Concerning the interactions with SIA1, it is observed (Table 2(a) and Fig. S1(a)) that the electrostatic interactions by charged residues dominate because SIA1 is negatively charged, while their magnitudes are somewhat overestimated due to the neglect of screening effect by solvent in the present FMO analysis. In addition, those residues such as Tyr98, Thr136 and Ser137 show strongly attractive interactions. As observed in Fig. 3(a) and (b), there are hydrogen bonding interactions with SIA1 by these and other (Ala135, Glu190 and Gln226) residues. As for the interactions with GAL2 part (Table 2(b) and Fig. S1(b)), Gln226 shows the strongest (attractive) interaction which is associated with the dispersion contribution as well as the hydrogen bonding with GAL2 (Fig. 3(c)). On the other hand, Glu190 shows the strongest (attractive) interaction with NAG3 (Table 2(c) and Fig. S1(c)).

Table 3
IFIEs (in units of kcal/mol) between each amino acid residue of H7N9 (human) HA and each part of avian receptor. (a) SIA1, (b) GAL2, (c) NAG3, and (d) GAL4. The MP2 value is given by the sum of the HF value and the correlation correction. Only the important interactions whose magnitudes are large or which play a vital role for binding are shown along with the charged state of the residues. See also Fig. S2 in Supplementary Information.

Residue	Charge	HF	Correlation	MP2
(a)				
ASP77	−	19.2	0.0	19.2
ASP95	−	16.4	0.0	16.4
LYS101	+	−17.1	0.0	−17.1
ARG131	+	−28.3	−0.1	−28.4
THR136		−23.1	−7.1	−30.2
SER137		−29.5	−2.8	−32.3
ARG140	+	−31.0	0.0	−31.0
ARG141	+	−25.1	0.0	−25.1
LYS152	+	−17.8	0.0	−17.8
ASP158	−	24.5	0.0	24.5
GLU190	−	26.0	−2.9	23.1
LYS193	+	−33.2	0.0	−33.2
LYS200	+	−16.9	0.0	−16.9
ARG220	+	−25.6	0.0	−25.6
ARG229	+	−31.6	−0.1	−31.7
ASP231	−	18.4	0.0	18.4
ASP255	−	15.4	0.0	15.4
TYR98		−7.3	−4.0	−11.4
ALA135		1.0	−1.0	0.0
(b)				
ARG131	+	1.4	0.0	1.4
ALA138		1.2	0.0	1.2
GLU190	−	−1.7	−0.1	−1.8
LYS193	+	1.7	0.0	1.7
LEU226		−1.4	−2.8	−4.2
(c)				
ASP77	−	−0.6	0.0	−0.6
SER137		0.7	0.0	0.7
ARG140	+	1.7	0.0	1.7
ARG141	+	1.0	0.0	1.0
GLN191		−0.6	0.0	−0.6
LYS193	+	−1.2	0.0	−1.2
GLN222		13.9	−4.6	9.3
VAL223		0.5	0.0	0.5
LEU226		−5.6	−0.7	−6.3
SER227		1.8	−0.2	1.6
GLY228		1.3	0.0	1.3
ARG229	+	1.0	0.0	1.0
(d)				
ARG220	+	−1.3	0.0	−1.3
GLN222		−2.0	−0.3	−2.3

Values in kcal/mol.

Next, Table 3 and Fig. S2 illustrate the IFIEs between amino acid residues of human (H7N9) HA and each part (SIA1, GAL2, NAG3 and GAL4) of avian receptor. Concerning the interactions with SIA1 (Table 3(a) and Fig. S2(a)), the contributions from the charged residues dominate again as well as in the case of H7N3, and the hydrogen bonds associated with Ala135, Thr136, Ser137, Tyr98 and Glu190 also play an important role (Fig. 4(a) and (b)). As for the interaction with GAL2 (Table 3(b) and Fig. S2(b)), the mutated Leu226 shows an attractive interaction in which the dispersion energy plays a vital role. The NAG3 shows the most attractive interaction with Leu226 (Table 3(c) and Fig. S2(c)), and forms a hydrogen bond with Gln222 (Fig. 4(c)) with inclusion of dispersion contribution. In addition, Arg220 and Gln222 show weakly attractive interactions with GAL4 (Table 3(d) and Fig. S2(d)).

Then, Table 4 and Fig. S3 illustrate the differences in IFIEs (ΔIFIE) with each saccharide part of the avian receptor between the corresponding residues of avian (H7N3) and human (H7N9) HAs. It is interesting for the interactions with SIA1 that, in addition

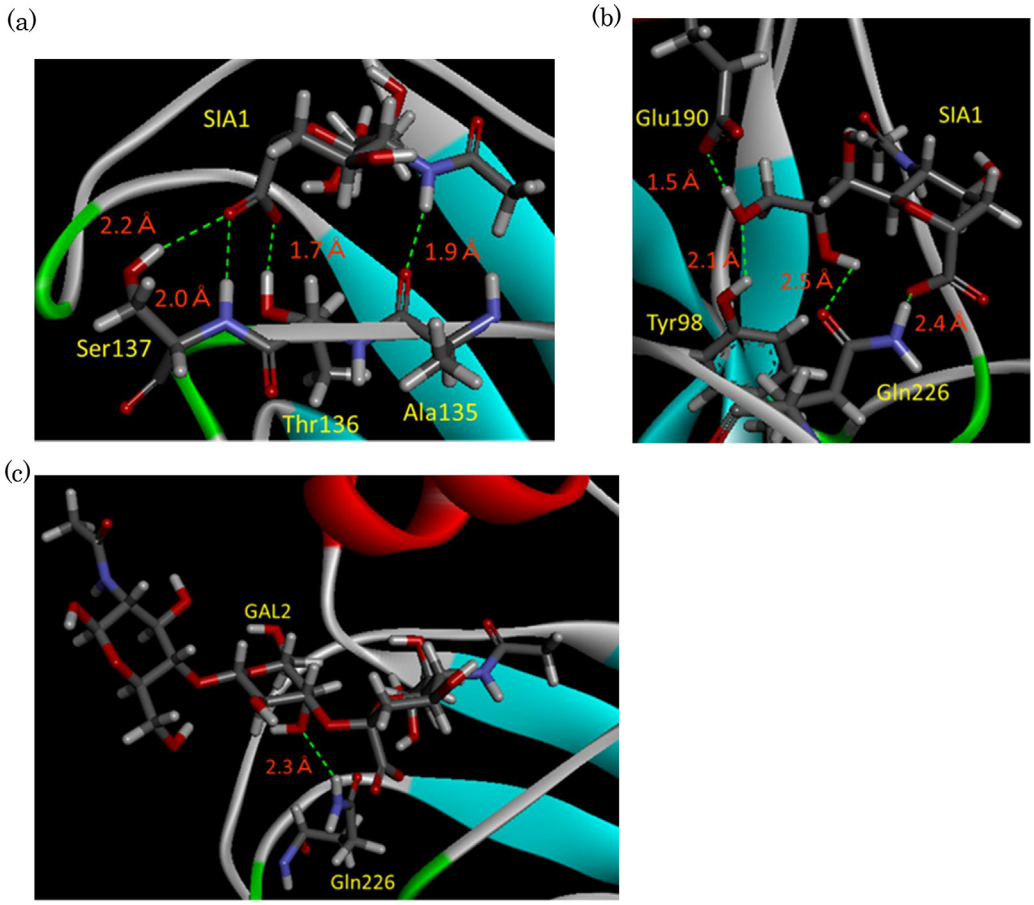

Fig. 3. Hydrogen bonds (represented by green dotted line with the distance marked in red) between amino acid residues of avian (H7N3) HA and avian receptor. (a and b) SIA1 part, and (c) GAL2 part. (For interpretation of the references to color in text, the reader is referred to the web version of this article.)

to mutated residues such as Asp174Ser, Gln226Leu, Asn298Asp and Glu312Arg, unmutated charged residues such as Arg140 and Glu190 show significant differences of interactions as well (Table 4(a) and Fig. S3(a)). To see the reason for it, we show in Fig. 5 that the orientations of guanidino group (and therefore the interactions with SIA1) of Arg140 are substantially different between H7N3 and H7N9. We have then investigated the interactions between Arg140 and other residues inside HAs (Table 5). We have thus found that there is a significant difference in IFIEs of Asp174Ser with Arg140 by 8.6 kcal/mol between H7N3 and H7N9, which should cause the orientational change of Arg140. Further, consequently, the interactions of Arg140 with Ala138, Ser142 and Gly144 have also been changed. This provides an interesting example that the intramolecular effects due to the mutation on the structural change of HA modify the HA-receptor interactions in an indirect manner; the mutation of Asp174Ser thus changes the HA-receptor interaction both directly and indirectly. In addition, it is noted that the mutations of Gln226Leu and Glu312Arg act in favor of the binding of human HA (H7N9) to the avian receptor, while the mutation Asn298Asp acts in the opposite way.

Table 4(b) and Fig. S3(b) show the comparison of the interactions with GAL2 part of avian receptor between H7N3 and H7N9 hemagglutinin residues. It is seen in Table 4(b) that there is a conversion

Table 4
Comparison of IFIEs (in units of kcal/mol) for each amino acid residue interacting with each part of avian receptor between H7N3 (avian) HA and H7N9 (human) HA calculated by the FMO-MP2/6-31G method. (a) SIA1, (b) GAL2 and (c) NAG3. Only the important interactions for binding are shown. Concerning the difference ΔIFIE between H7N3 (avian) HA and H7N9 (human) HA, see also Fig. S3 in Supplementary Information.

Residue	H7N3 (avian)	H7N9 (human)	ΔIFIE
(a)			
ARG140	−25.8	−31.0	5.1
ASP174SER	8.4	−0.2	8.6
GLU190	17.6	23.1	−5.5
GLN226LEU	12.9	−2.5	15.4
ASN298ASP	0.2	8.5	−8.4
GLU312ARG	6.3	−6.0	12.3
(b)			
GLU190	1.3	−1.8	3.1
LYS193	0.4	1.7	−1.3
ARG220	−0.5	0.7	−1.1
GLY225	0.2	−1.0	1.2
(c)			
GLN222	−0.2	9.3	−9.5
GLN226LEU	−0.2	−6.3	6.1

Values in kcal/mol.

Table 5
IFIEs (in units of kcal/mol) between Arg140 and other residues in HA of H7N3 (avian) or H7N9 (human) in complex with avian receptor. Only the important interactions for which the difference ΔIFIE between H7N3 (avian) HA and H7N9 (human) HA is large are shown.

Residue	H7N3 (avian)	H7N9 (human)	ΔIFIE
ALA138	−11.7	−25.2	13.5
SER142	4.4	−3.2	7.7
GLY144	5.4	−1.6	7.1
ASP174SER	−8.4	0.2	−8.6

Values in kcal/mol.

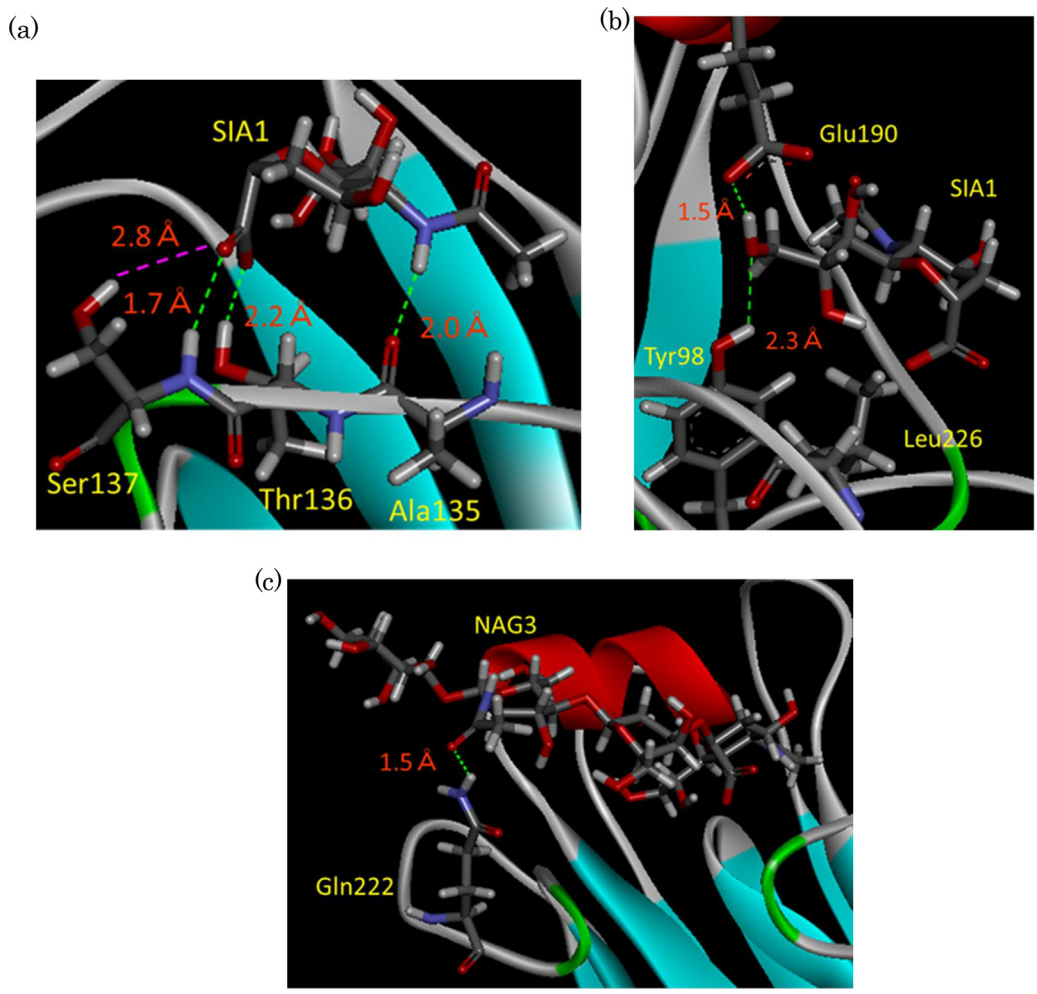

Fig. 4. Hydrogen bonds (represented by green dotted line with the distance marked in red) between amino acid residues of human (H7N9) HA and avian receptor. (a and b) SIA1 part, and (c) NAG3 part. (For interpretation of the references to color in text, the reader is referred to the web version of this article.)

from repulsive to attractive interactions with Glu190. Shi et al. [22] pointed out that a hydrophobic pocket is formed by Ala138, Val186, Pro221 and Leu226 in human (H7N9) HA due to the mutations of Gly186Val and Gln226Leu, which, in turn, makes the hydroxymethyl group of GAL2 rotate toward the 130-loop (Fig. 6), thus leading to the change in the interaction with Glu190. In addition, the interactions of GAL2 with Lys193, Arg220 and Gly225 are modified as well, which may also be regarded as indirect effects. Further, Table 4(c) and Fig. S3(c) show the comparison of the interactions with NAG3 part of avian receptor between H7N3 and H7N9 hemagglutinin residues. As seen in Table 4(c), the mutation Gln226Leu makes the interaction between the human HA (H7N9) and the avian receptor more attractive as in the case of SIA1. This causes the change of the location of the saccharide receptor (Fig. 7), thus making the interaction between NAG3 and Gln222 more repulsive in the case of H7N9.

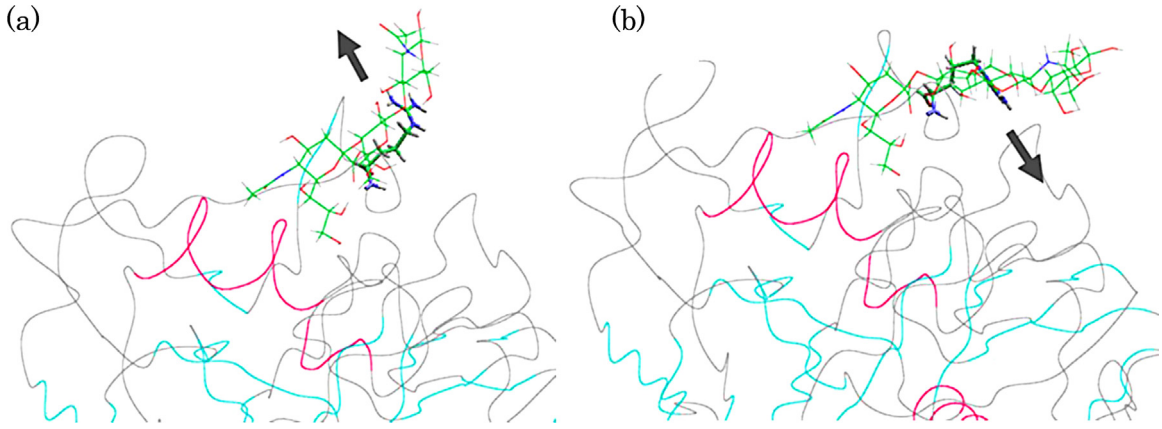

Fig. 5. Orientations of Arg140 of (a) avian (H7N3) HA and (b) human (H7N9) HA in complex with avian receptor.

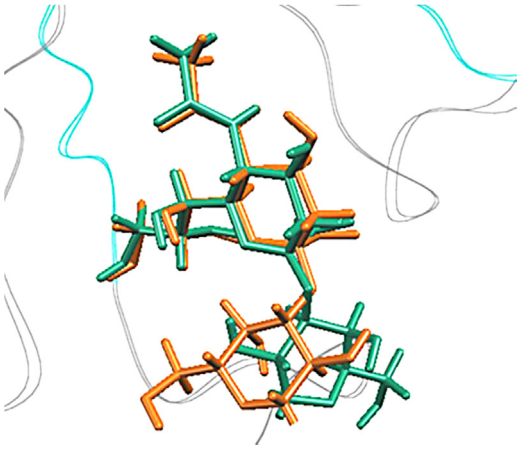

Fig. 6. Conformations of GAL2 of avian receptor in complex with avian HA (orange) and human HA (green). (For interpretation of the references to color in text, the reader is referred to the web version of this article.)

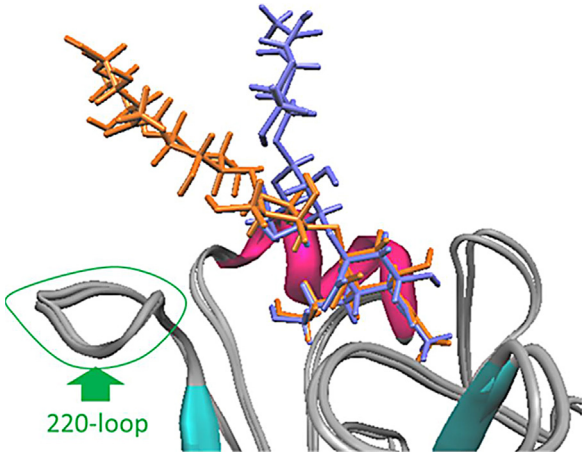

Fig. 7. Conformations of NAG3 of avian receptor in complex with human HA (orange) and avian HA (blue). (For interpretation of the references to color in text, the reader is referred to the web version of this article.)

As observed above, the interactions of avian and human HAs with the avian receptor change significantly at Arg140, Glu190 and Gln222 in spite of the fact that these amino acid residues are not mutated. This is a kind of indirect effect which demonstrates the importance of intramolecular (and intermolecular) structural changes caused by the mutations at other amino acid sites. Taking account of all these interactions, the human HA (H7N9) keeps a moderate binding to the avian receptor even after the mutations relative to the avian HA (H7N3).

3.3. Interactions between HA proteins and human receptor

In this section we investigate the interactions between the HA proteins and the human type α2–6 receptor, through which the reason why H7N9 has acquired the transmission ability to human cells will be elucidated at molecular level. As seen in Table 1, the attractive interaction between the avian HA (H7N3) and the SIA1 part of human receptor is the weakest among the four complexes considered in the present study. By transforming into the human HA (H7N9), there is a gain of the attractive interaction by 20.6 kcal/mol. Table 6 and Fig. S4 illustrate the IFIEs between amino acid residues of avian (H7N3) HA and each part (SIA1 and GAL2) of human receptor. In addition to some charged residues, Thr136 and Ser137 of avian HA show strongly attractive interactions with SIA1 (Table 6(a) and Fig. S4(a)). Tyr98 also shows an attractive interaction by −9.9 kcal/mol, which may be associated with the hydrogen bond and van der Waals interactions. Fig. 8 illustrates hydrogen bonds with SIA1 formed by Ala135, Thr136, Ser137, Tyr98 and Gln226. On the other hand, as seen in Table 6(b) and Fig. S4(b), Glu190 and Gln226 show considerably attractive interactions with GAL2, where a relatively strong dispersion interaction (−2.9 kcal/mol) is observed for Gln226. However, on the whole, the attractive interactions between the avian HA and the human receptor are not so strong in comparison with other complexes.

Table 7 and Fig. S5 illustrate the IFIEs between amino acid residues of human (H7N9) HA and each part (SIA1 and GAL2) of human receptor. Analogous to the case of H7N3, Thr136 and Ser137 of human HA show strongly attractive interactions with SIA1 as well as charged amino acid residues. Fig. 9 illustrates hydrogen bonds with SIA1 formed by Ala135, Thr136, Ser137, Tyr98 and Glu190. On the other hand, the mutated Leu226 shows an attractive interaction by −5.9 kcal/mol with GAL2, where a dispersion interaction due to the electron correlation is also observed by −1.7 kcal/mol. Glu190 also shows an attractive interaction with GAL2 by −3.8 kcal/mol.

Here let us compare the interactions of avian and human HAs with the human receptor. Table 8 and Fig. S6 illustrate the differences in IFIEs (ΔIFIE) with each saccharide part (SIA1 and GAL2) of the human receptor between the corresponding residues of avian (H7N3) and human (H7N9) HAs. As seen in Table 8(a) and Fig. S6(a), there are substantial differences in the interaction energies with SIA1 for Arg140, Asp174Ser, Glu190, Asn298Asp and Glu312Arg. The mutations to more positively charged residues would be

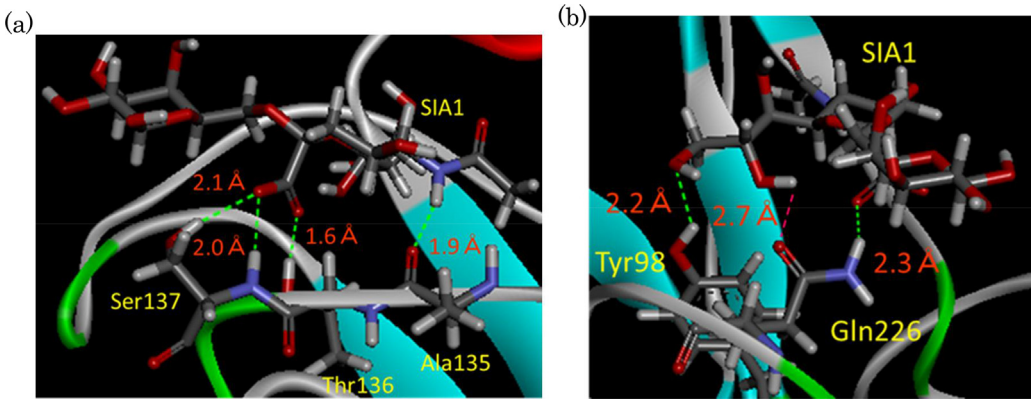

Fig. 8. (a and b) Hydrogen bonds (represented by green dotted line with the distance marked in red) between amino acid residues of avian (H7N3) HA and SIA1 part of human receptor. (For interpretation of the references to color in text, the reader is referred to the web version of this article.)

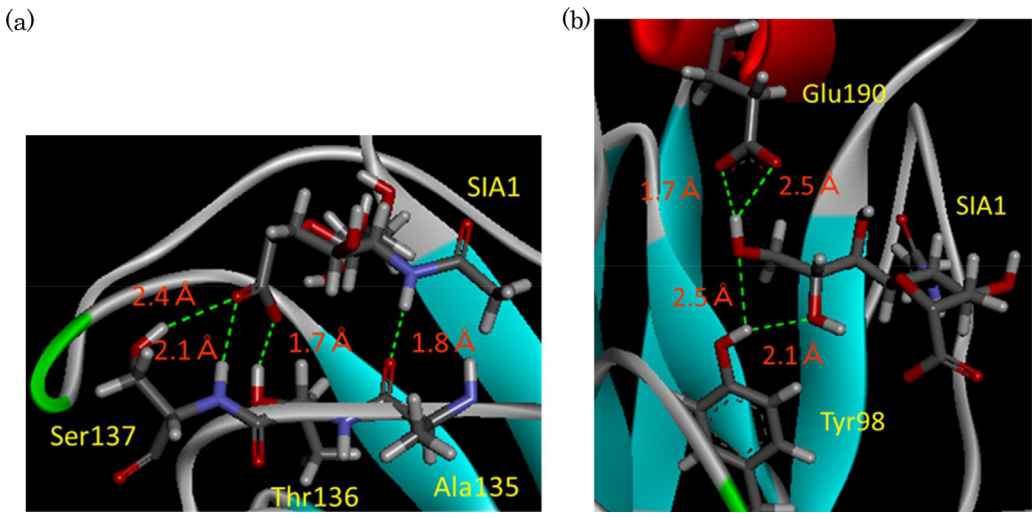

Fig. 9. (a and b) Hydrogen bonds (represented by green dotted line with the distance marked in red) between amino acid residues of human (H7N9) HA and SIA1 part of human receptor. (For interpretation of the references to color in text, the reader is referred to the web version of this article.)

favorable for the binding to SIA1 since the SIA1 part is negatively charged. Further, we focus on the significant contributions by Arg140 and Glu190 which are not mutated. Table 9 illustrates the IFIEs between Arg140 and other residues inside the avian and human HAs. It is observed in this table that there are significant differences in IFIEs of Arg140 for Asp174Ser and Ser145. Due to these differences associated with the mutation of Asp174Ser, Arg140 is attracted to Asp174 in the case of avian HA, while Arg140 is attracted to neighboring Ser145 in the case of human HA. Thus, in the case of human HA, the side chain of Arg140 is directed toward Ser145, leading to the orientational change of Arg140 and consequently to the more attractive change in the IFIE with SIA1 by −7.3 kcal/mol (see Fig. 10). Further, the orientation of Glu190 is also changed between avian and human HAs, as seen in Fig. 11. To see the reason for it, we have analyzed the IFIEs between Glu190 and other residues inside the HAs and found that the interactions with Gly186Val are remarkably different between the avian and human HAs; the IFIE between Glu190 and Gly186 is −5.0 kcal/mol in the case of avian HA (H7N3), while that between Glu190 and Val186 is −24.3 kcal/mol in the case of human HA (H7N9). Thus, the carboxyl group of Glu190 is directed toward Val186 in the case of human HA (Fig. 11), which causes the formation of a hydrogen bond between Glu190 and the side chain of SIA1, substantially mitigating the electrostatic repulsion observed in the case of avian HA.

On the other hand, as for the interactions with GAL2 part of the human receptor, Arg140, Asp158, Lys193, Gln222 and Gln226Leu show large differences in IFIEs between the avian and human HAs

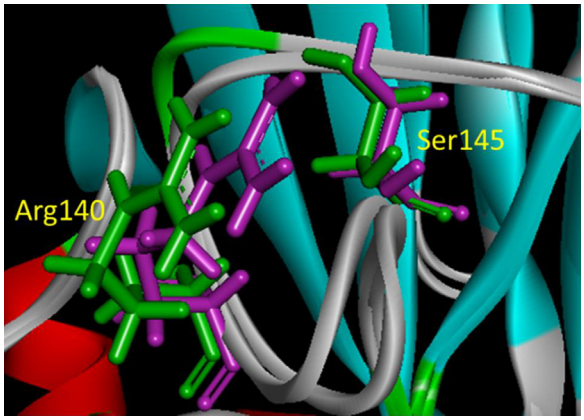

Fig. 10. Orientations of Arg140 and Ser145 of avian (H7N3) HA (green) and human (H7N9) HA (magenta) in complex with human receptor. (For interpretation of the references to color in text, the reader is referred to the web version of this article.)

(Table 8(b) and Fig. S6(b)). The hydrophobic pocket formed by Ala138, Val186 and Leu226 in the human HA (H7N9) again play an important role [23,42], which alters the conformation of GAL2 significantly, as seen in Fig. 12. This conformational change, in turn, brings about the changes of interaction energies between GAL2 and HA residues, especially for charged or polar residues, even if they

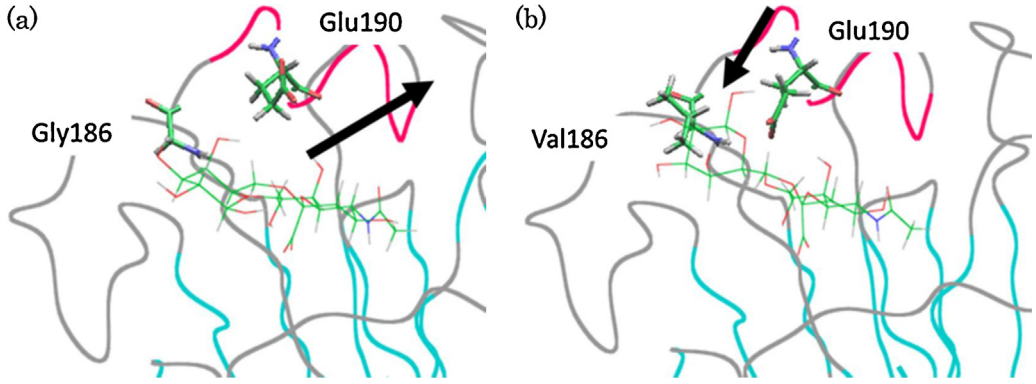

Fig. 11. Orientations of Glu190 of (a) avian (H7N3) HA and (b) human (H7N9) HA in complex with human receptor.

Table 6
IFIEs (in units of kcal/mol) between each amino acid residue of H7N3 (avian) HA and each part of human receptor. (a) SIA1 and (b) GAL2. The MP2 value is given by the sum of the HF value and the correlation correction. Only the important interactions whose magnitudes are large or which play a vital role for binding are shown along with the charged state of the residues. See also Fig. S4 in Supplementary Information.

Residue	Charge	HF	Correlation	MP2
(a)				
ASP77	−	18.4	0.0	18.4
ASP95	−	16.0	0.0	16.0
LYS101	+	−17.2	0.0	−17.2
ARG131	+	−27.3	0.0	−27.3
THR136		−26.5	−7.1	−33.7
SER137		−36.3	−4.1	−40.5
ARG140	+	−31.2	0.0	−31.2
ARG141	+	−24.3	0.0	−24.3
LYS152	+	−17.3	0.0	−17.3
ASP158	−	28.5	0.0	28.5
GLU190	−	34.7	−1.1	33.6
LYS193	+	−35.5	−0.2	−35.7
LYS200	+	−17.9	0.0	−17.9
ARG220	+	−27.9	0.0	−27.9
ARG229	+	−32.4	−0.1	−32.5
ASP231	−	19.1	0.0	19.1
ASP255	−	15.1	0.0	15.1
TYR98		−6.2	−3.7	−9.9
ALA135		2.0	−1.2	0.8
(b)				
ARG131	+	1.8	0.0	1.8
THR136		−1.4	−0.4	−1.7
ALA138		1.5	0.0	1.5
ARG140	+	−1.5	0.0	−1.5
LYS152	+	1.0	0.0	1.0
ASP158	−	−1.3	0.0	−1.3
GLU190	−	−3.5	0.0	−3.5
LYS193	+	1.8	0.0	1.8
LYS200	+	1.1	0.0	1.1
ARG220	+	2.0	0.0	2.0
GLN226		−6.3	−2.9	−9.2
SER227		1.3	0.0	1.3
ARG229	+	2.4	0.0	2.4
ASP231	−	−1.2	0.0	−1.2

Values in kcal/mol.

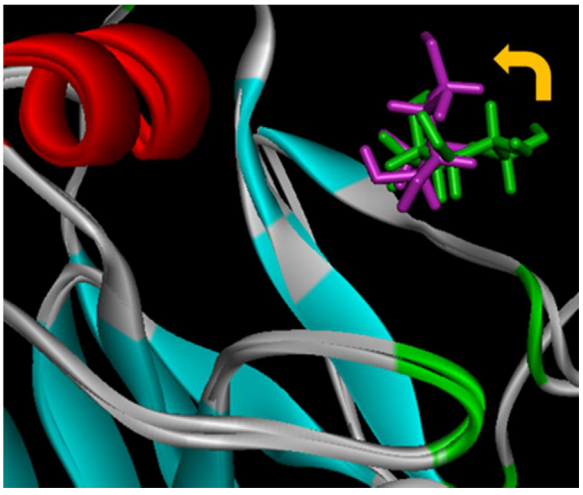

Fig. 12. Conformations of GAL2 of human receptor in complex with avian HA (green) and human HA (magenta). (For interpretation of the references to color in text, the reader is referred to the web version of this article.)

Table 7
IFIEs (in units of kcal/mol) between each amino acid residue of H7N9 (human) HA and each part of human receptor. (a) SIA1 and (b) GAL2. The MP2 value is given by the sum of the HF value and the correlation correction. Only the important interactions whose magnitudes are large or which play a vital role for binding are shown along with the charged state of the residues. See also Fig. S5 in Supplementary Information.

Residue	Charge	HF	Correlation	MP2
(a)				
ASP77	−	19.4	0.0	19.4
ASP95	−	16.5	0.0	16.5
LYS101	+	−17.4	0.0	−17.4
GLU105	−	15.0	0.0	15.0
ARG131	+	−26.5	0.0	−26.5
THR136		−24.3	−8.1	−32.4
SER137		−32.4	−3.7	−36.1
ARG140	+	−38.5	0.0	−38.5
ARG141	+	−25.9	0.0	−25.9
GLU150	−	15.0	0.0	15.0
LYS152	+	−18.5	0.0	−18.5
ASP158	−	24.1	0.0	24.1
LYS193	+	−32.1	0.0	−32.1
LYS200	+	−16.5	0.0	−16.5
ARG220	+	−25.9	0.0	−25.9
ARG229	+	−31.8	−0.1	−31.9
ASP231	−	18.3	0.0	18.3
ASP255	−	15.5	0.0	15.5
ARG256	+	−15.1	0.0	−15.1
TYR98		−6.1	−4.0	−10.2
ALA135		2.0	−1.5	0.4
(b)				
SER137		1.8	−0.3	1.5
ARG140	+	1.6	0.0	1.6
ARG141	+	1.4	0.0	1.4
GLU190	−	−3.7	0.0	−3.8
ARG220	+	1.2	0.0	1.2
LEU226		−4.2	−1.7	−5.9
ARG229	+	1.7	0.0	1.7

Values in kcal/mol.

Table 8
Comparison of IFIEs (in units of kcal/mol) for each amino acid residue interacting with each part of avian receptor between H7N3 (avian) HA and H7N9 (human) HA calculated by the FMO-MP2/6-31G method. (a) SIA1 and (b) GAL2. Only the important interactions for binding are shown. Concerning the difference ΔIFIE between H7N3 (avian) HA and H7N9 (human) HA, see also Fig. S6 in Supplementary Information.

Residue	H7N3 (avian)	H7N9 (human)	ΔIFIE
(a)			
ARG140	−31.2	−38.5	7.3
ASP174SER	8.4	−0.3	8.7
GLU190	33.6	14.6	19.0
ASN298ASP	0.2	8.6	−8.4
GLU312ARG	6.2	−6.0	12.2
(b)			
ARG140	−1.5	1.6	−3.1
ASP158	−1.3	−0.3	−1.0
LYS193	1.8	0.4	1.4
GLN222	−0.9	0.3	−1.2
GLN226LEU	−9.2	−5.9	−3.2

Values in kcal/mol.

Table 9
IFIEs (in units of kcal/mol) between Arg140 and other residues in HA of H7N3 (avian) or H7N9 (human) in complex with human receptor. Only the important interactions for which the difference ΔIFIE between H7N3 (avian) HA and H7N9 (human) HA is large are shown.

Residue	H7N3 (avian)	H7N9 (human)	ΔIFIE
SER142	3.4	−3.5	6.8
GLY144	1.7	−4.1	5.8
SER145	−4.6	−17.3	12.7
ASP174SER	−8.4	0.2	−8.6

Values in kcal/mol.

are not mutated. This may also be regarded as an indirect effect, as addressed above.

4. Conclusions

In this study we have performed the FMO-IFIE analysis for the intermolecular interactions between amino acid residues of avian or human HA protein and each part of avian or human saccharide receptor in order to elucidate the molecular mechanism of avian-to-human infectious transmission of influenza virus. It has thus been found that the human (H7N9) HA has a stronger binding affinity to the human receptor than the avian (H7N3) HA, while retaining a relatively strong affinity with the avian receptor, which is consistent with experimental observations [22,23]. Our calculated results also agree with the experimental results by Zhou et al. [42] demonstrating that H7N9 virus (A/Anhui/1/2013) binds to both avian-type and human-type receptors, in which Val186 and Leu226 of HA play vital roles. We have further investigated the molecular origins for these binding properties in details and revealed the importance of structural changes of the HA-receptor complexes caused by the mutations (indirect effect) as well as the importance of the modification of interactions between the mutated residues and the receptors (direct effect). For instance, to enhance the binding to SIA1, the mutations Asp174Ser and Glu312Arg make the direct contributions, while the mutations Asp174Ser and Gly186Val make the indirect contributions through the interactions with Arg140 and Glu190, respectively. Moreover, to understand the significance of the indirect effect in these HA-receptor complex systems, it may also be supposed that intrinsic flexibilities of sialosaccharide chain play a vital role, whose quantitative elucidation remains a theoretical challenge in a biological context. In any event we can now perform structure-based theoretical analyses of the binding affinity of HA-receptor complexes in terms of accurate quantum-chemical calculations, which would provide useful information for the prediction of possible interspecies transmission associated with influenza pandemic and the development of influenza vaccines against target HA proteins with forthcoming mutations. It is also noted that reliable structure data for the HA-receptor complexes are essential in these theoretical analyses. We are currently at a position that we can exploit all the tools from virology, structural biology and computational chemistry in order to prepare for the threat of influenza pandemic.

Acknowledgment

This work was partially supported by “Research and Development of Innovative Simulation Software” project at Institute of Industrial Science, the University of Tokyo.

Appendix A. Supplementary data

Supplementary data associated with this article can be found, in the online version, at http://dx.doi.org/10.1016/j.jmgm.2014.07.004.

References

[1] R.S. Daniels, A.R. Douglas, J.J. Skehel, D.C. Wiley, Analyses of the antigenicity of influenza haemagglutinin at the pH optimum for virus-mediated membrane fusion, J. Gen. Virol. 64 (1983) 1657–1662.
[2] D.C. Wiley, The structure and function of the hemagglutinin membrane glycoprotein of influenza virus, Annu. Rev. Biochem. 56 (1987) 365–394.
[3] J.J. Skehel, D.C. Wiley, Receptor binding and membrane fusion in virus entry: the influenza hemagglutinin, Annu. Rev. Biochem. 69 (2000) 531–569.
[4] J.B. Poltkin, J. Dushoff, S.A. Levin, Hemagglutinin sequence clusters and the antigenic evolution of influenza A virus, Proc. Natl. Acad. Sci. U. S. A. 99 (2002) 6236–6268.
[5] K. Nakajima, E. Nobusawa, A. Nagy, S. Nakajima, Accumulation of amino acid substitutions promotes irreversible structural changes in the hemagglutinin of human influenza AH3 virus during evolution, J. Virol. 79 (2005) 6472–6477.
[6] A.I. Karasin, M.M. Schutten, L.A. Cooper, C.B. Smith, K. Subbarao, G.A. Anderson, S. Carman, C.W. Olsen, Genetic characterization of H3N2 influenza viruses isolated from pigs in North America, 1977–1999: evidence for wholly human and reassortant virus genotypes, Virus Res. 68 (2000) 71–85.
[7] Y. Suzuki, Sialobiology of influenza: molecular mechanism of host range variation of influenza viruses, Biol. Pharm. Bull. 28 (2005) 399–408.
[8] C.R. Parrish, Y. Kawaoka, The origins of new pandemic viruses: the acquisition of new host ranges by canine parvovirus and influenza A viruses, Annu. Rev. Microbiol. 59 (2005) 553–586.
[9] T. Horimoto, Y. Kawaoka, Influenza: lessons from past pandemics, warnings from current incidents, Nat. Rev. Microbiol. 3 (2005) 591–600.
[10] G. Neumann, Y. Kawaoka, Host range restriction and pathogenicity in the context of influenza pandemic, Emerg. Infect. Dis. 12 (2006) 881–886.
[11] T. Iwata, K. Fukuzawa, K. Nakajima, S. Aida-Hyugaji, Y. Mochizuki, H. Watanabe, S. Tanaka, Theoretical analysis of binding specificity of influenza viral hemagglutinin to avian and human receptors based on the fragment molecular orbital method, Comput. Biol. Chem. 32 (2008) 198–211.
[12] K. Fukuzawa, K. Omagari, K. Nakajima, E. Nobusawa, S. Tanaka, Sialic acid recognition of the pandemic influenza 2009 H1N1 virus: binding mechanism between human receptor and influenza hemagglutinin, Protein Pept. Lett. 18 (2011) 530–539.
[13] K. Kitaura, E. Ikeo, T. Asada, T. Nakano, M. Uebayasi, Fragment molecular orbital method: an approximate computational method for large molecules, Chem. Phys. Lett. 313 (1999) 701–706.
[14] D.G. Fedorov, K. Kitaura, Extending the power of quantum chemistry to large systems with the fragment molecular orbital method, J. Phys. Chem. A 111 (2007) 6904–6914.
[15] K. Takematsu, K. Fukuzawa, K. Omagari, S. Nakajima, K. Nakajima, Y. Mochizuki, T. Nakano, H. Watanabe, S. Tanaka, Possibility of mutation prediction of influenza hemagglutinin by combination of hemadsorption experiment and quantum chemical calculation for antibody binding, J. Phys. Chem. B 113 (2009) 4991–4994.
[16] T. Sawada, D.G. Fedorov, K. Kitaura, Role of the key mutation in the selective binding of avian and human influenza hemagglutinin to sialosides revealed by quantum-mechanical calculations, J. Am. Chem. Soc. 132 (2010) 16862–16872.
[17] T. Sawada, D.G. Fedorov, K. Kitaura, Binding of influenza A virus hemagglutinin to the sialoside receptor is not controlled by the homotropic allosteric effect, J. Phys. Chem. B 114 (2010) 15700–15705.
[18] A. Yoshioka, K. Fukuzawa, Y. Mochizuki, K. Yamashita, T. Nakano, Y. Okiyama, E. Nobusawa, K. Nakajima, S. Tanaka, Prediction of probable mutations in influenza virus hemagglutinin protein based on large-scale ab initio fragment molecular orbital calculations, J. Mol. Graph. Model. 30 (2011) 110–119.
[19] S. Tanaka, Y. Mochizuki, Y. Komeiji, Y. Okiyama, K. Fukuzawa, Electron-correlated fragment-molecular-orbital calculations for biomolecular and nano systems, Phys. Chem. Chem. Phys. 16 (2014) 10310–10344.
[20] Y. Chen, et al., Human infections with the emerging avian influenza A H7N9 virus from wet market poultry: clinical analysis and characterisation of viral genome, Lancet 381 (2013) 1916–1925.
[21] R. Gao, et al., Human infection with a novel avian-origin influenza A (H7N9) virus, N. Engl. J. Med. 368 (2013) 1888–1897.
[22] Y. Shi, W. Zhang, F. Wang, J. Qi, Y. Wu, H. Song, F. Gao, Y. Bi, Y. Zhang, Z. Fan, C. Qin, H. Sun, J. Liu, J. Haywood, W. Liu, W. Gong, D. Wang, Y. Shu, Y. Wang, J. Yan, G.F. Gao, Structures and receptor binding of hemagglutinins from human-infecting H7N9 influenza viruses, Science 342 (2013) 243–247.
[23] X. Xiong, S.R. Martin, L.F. Haire, S.A. Wharton, R.S. Daniels, M.S. Bennett, J.W. Mccauley, P.J. Collins, P.A. Walker, J.J. Skehel, S.J. Gamblin, Receptor binding by an H7N9 influenza virus from humans, Nature 499 (2013) 496–499.
[24] J. Wang, P. Cieplak, P.A. Kollman, How well does a restrained electrostatic potential (RESP) model perform in calculating conformational energies of organic and biological molecules, J. Comput. Chem. 21 (2000) 1049–1074.
[25] K. Fukuzawa, Y. Mochizuki, S. Tanaka, K. Kitaura, T. Nakano, Molecular interactions between estrogen receptor and its ligand studied by ab initio fragment molecular orbital method, J. Phys. Chem. B 110 (2006) 16102–16110.
[26] Y. Okiyama, K. Fukuzawa, H. Yamada, Y. Mochizuki, T. Nakano, S. Tanaka, Counterpoise-corrected interaction energy analysis based on the fragment molecular orbital scheme, Chem. Phys. Lett. 509 (2011) 67–71.
[27] X. He, L. Fusti-Molnar, G. Cui, K.M. Merz Jr., Importance of dispersion and electron correlation in ab initio protein folding, J. Phys. Chem. B 113 (2009) 5290–5300.
[28] Y. Ding, Y. Mei, J.Z.H. Zhang, Quantum mechanical studies of residue-specific hydrophobic interactions in p53-MDM2 binding, J. Phys. Chem. B 112 (2008) 11396–11401.
[29] K. Fukuzawa, Y. Komeiji, Y. Mochizuki, A. Kato, T. Nakano, S. Tanaka, Intra- and intermolecular interaction between cyclic-AMP receptor protein and DNA: ab initio fragment molecular orbital study, J. Comput. Chem. 27 (2006) 948–960.
[30] M. Ito, K. Fukuzawa, Y. Mochizuki, T. Nakano, S. Tanaka, Ab initio fragment molecular orbital study of molecular interactions between liganded retinoid X receptor and its coactivator: roles of helix 12 in the coactivator binding mechanism, J. Phys. Chem. B 111 (2007) 3525–3533.
[31] I. Kurisaki, K. Fukuzawa, Y. Komeiji, Y. Mochizuki, T. Nakano, J. Imada, A. Chmielewski, S.M. Rothstein, H. Watanabe, S. Tanaka, Visualization analysis of inter-fragment interaction energies of CRP-cAMP-DNA complex based on the fragment molecular orbital method, Biophys. Chem. 130 (2007) 1–9.

[32] C. Watanabe, K. Fukuzawa, Y. Okiyama, T. Tsukamoto, A. Kato, S. Tanaka, Y. Mochizuki, T. Nakano, Three- and four-body corrected fragment molecular orbital calculations with a novel subdividing fragmentation method applicable to structure-based drug design, J. Mol. Graph. Model. 41 (2013) 31–42.
[33] H. Watanabe, S. Tanaka, N. Okimoto, A. Hasegawa, M. Taiji, Y. Tanida, T. Mitsui, M. Katsuyama, H. Fujitani, Comparison of binding affinity evaluations for FKBP ligands with state-of-the-art computational methods: FMO, QM/MM, MM-PB/SA, and MP-CAFEE approaches, Chem-Bio Inform. J. 10 (2010) 32–45.
[34] H. Watanabe, Y. Okiyama, T. Nakano, S. Tanaka, Incorporation of solvation effects into fragment molecular orbital calculation with the Poisson–Boltzmann equation, Chem. Phys. Lett. 500 (2010) 116–119.
[35] S. Tanaka, C. Watanabe, Y. Okiyama, Statistical correction to effective interactions in the fragment molecular orbital method, Chem. Phys. Lett. 556 (2013) 272–277.
[36] M.P. Mazanetz, O. Ichihara, R.J. Law, M. Whittaker, Prediction of cyclin-dependent kinase 2 inhibitor potency using the fragment molecular orbital method, J. Cheminform. 3 (2011) 2.
[37] S.A. Hayik, R. Dunbrack Jr., K.M. Merz Jr., A mixed QM/MM scoring function to predict protein–ligand binding affinity, J. Chem. Theory Comput. 6 (2010) 3079–3091.
[38] H. Yang, P.J. Carney, R.O. Donis, J. Stevens, Structure and receptor complexes of the hemagglutinin from a highly pathogenic H7N7 influenza virus, J. Virol. 86 (2012) 8645–8652.
[39] ClustalW ver. 1.83, http://clustalw.ddbj.nig.ac.jp
[40] R. Xu, R.P. de Vries, X. Zhu, C.M. Nycholat, R. McBride, W. Yu, J.C. Paulson, I.A. Wilson, Preferential recognition of avian-like receptors in human influenza A H7N9 viruses, Science 342 (2013) 1230–1235.
[41] M. Li, B. Wang, Computational studies of H5N1 hemagglutinin binding with SA-α-2,3-Gal and SA-α-2,6-Gal, Biochem. Biophys. Res. Commun. 347 (2006) 662–668.
[42] J. Zhou, et al., Biological features of novel avian influenza A (H7N9) virus, Nature 499 (2013) 500–503.